

Róbert SOBOTA , Ladislav MOROVIČ ,
Mária KAPUSTOVÁ , Jozef BÍLIK 

Slovak University of Technology in Bratislava, Faculty of Materials Science and Technology in Trnava,
Slovak Republic

Peter BELLA, Milan MOJŽIŠ

ŽP Research and Development Centre, Podbrezová, Slovak Republic

Forming 2022

ANALYSIS AND COMPARISON OF GEOMETRIC DIMENSIONS OF COLD DRAWN TUBES USING FEM SIMULATION

ANALIZA I PORÓWNANIE WYMIARÓW GEOMETRYCZNYCH RUR CIĄGNIONYCH NA ZIMNO Z WYKORZYSTANIEM SYMULACJI MES

The paper focuses on the analysis and comparison of tube wall thickness after cold drawing. The tube wall thickness obtained by the experiment was compared with the wall thickness obtained using finite element method (FEM) simulation in the simulation software DEFORM-3D. For the experiment the tube sinking technology was performed and all tubes were made of steel E235. Tubes were the outer diameter of $\varnothing 14$, $\varnothing 16$, $\varnothing 18$ mm and the tube wall thickness was 1 and 2 mm. All tubes were drawn by single-pass tube sinking technology to the final diameter of $\varnothing 12$ mm. Tube sinking process is a tube drawing technology through a drawing die without the use of a mandrel. Tube sinking is used as a final drawing operation, especially in the production of precision tubes of smaller diameter. The resulting comparison showed that the tube wall thickness obtained by the simulation in the DEFORM software very well matches with tube wall thickness obtained in the experiments. Based on the results, it can be stated that in the future it will be possible to replace some of the real experiments with FEM simulation in the DEFORM software.

Keywords: FEM simulation, simulation software DEFORM, cold tubes drawing, seamless tubes, drawing tool, sinking drawing process

Niniejszy artykuł poświęcono analizie i porównaniu grubości ścianek rur po ciągnięciu na zimno. Grubość ścianki rury uzyskaną w eksperymencie porównano z grubością ścianki uzyskaną za pomocą symulacji metodą elementów skończonych (MES) przy użyciu oprogramowania symulacyjnego DEFORM-3D. W eksperymencie wykorzystano technologię zanurzania rur, a wszystkie rury wykonano ze stali E235. Rury miały średnicę zewnętrzną $\varnothing 14$, $\varnothing 16$, $\varnothing 18$ mm, a grubość ścianki rury wynosiła 1 i 2 mm. Wszystkie rury były ciągnięte w jednym ciągu bez użycia trzpienia na końcową średnicę $\varnothing 12$ mm. Proces ciągnięcia swobodnego rur to technologia ciągnięcia rur za pomocą ciągnadła bez użycia trzpienia. Swobodne ciągnięcie rur jest stosowane jako ostatnia operacja procesu, zwłaszcza przy produkcji rur precyzyjnych o mniejszych średnicach. Porównanie wykazało, że grubość ścianki rury uzyskana w symulacji przy użyciu programu DEFORM bardzo dobrze koreluje z grubością ścianki rury uzyskanej w eksperymentach. Na podstawie uzyskanych wyników można stwierdzić, że w przyszłości możliwe będzie zastąpienie części eksperymentów rzeczywistych, symulacją MES przy użyciu oprogramowania DEFORM.

Słowa kluczowe: symulacja MES, oprogramowanie symulacyjne DEFORM, ciągnięcie rur na zimno, rury bezszwowe, narzędzie do ciągnięcia, proces ciągnięcia swobodnego

1. INTRODUCTION

Cold tubes drawing technology is used to process metals and alloys with good or poorer formability, while the tube production is influenced by various process parameters, i.e. mostly die geometry, degree of deformation and rate of deformation, force conditions, friction conditions, method of lubrication and

type of lubricant used. Cold tubes drawing is realized without use of mandrel (tube sinking) or with use of mandrel (mandrel drawing).

Cold tube drawing is one of the very common methods used for the production of seamless tubes, which are widely used especially in the engineering industry. The drawing process is performed by the tool called drawing die, which consists of three parts:

Corresponding Author: Róbert Sobota, email: robert.sobota@stuba.sk
Slovak University of Technology in Bratislava, Faculty of Materials Science and Technology in Trnava,
Bottova 25, 917 24 Trnava, Slovak Republic

the inlet part (i.e. reduction part), calibration part (i.e. cylindrical part) and outlet part. The calibration cylindrical part is placed between the reduction part and the outlet cone, on which the accuracy of the final diameter of the drawn tube depends. Tool geometry is therefore a very important parameter in the production of cold drawn tubes and affects the energy intensity of production as well as tool life [1–5].

The shape and dimensions of the die are the key factor in meeting the requirements for the geometric accuracy of the tube and the roughness of its surface. Many scientific outputs are available aimed at die shape optimizing and monitoring the influence of the die geometry on the final quality of production of precision tubes using finite element (FE) analysis [6–9].

FE analysis makes it possible to optimize technological parameters and predict their possible effects on the production quality of drawn tubes, as stated in the sources [10–14]. The scientific contribution of numerical simulation for the further development of tube sinking has also been proven in the contributions [6, 15, 16].

2. DESCRIPTION AND IMPLEMENTATION OF THE EXPERIMENT

Inlet tubes with outer diameter of $\varnothing 14$, $\varnothing 16$, $\varnothing 18$ mm and with wall thickness of $s = 1$ mm and 2 mm were used for the cold tube drawing experiment in laboratory conditions, which were drawn to the final outer diameter of $\varnothing 12$ mm by single-pass drawing technology. By drawing from the diameter of $\varnothing 14$, $\varnothing 16$, $\varnothing 18$ mm to the diameter of $\varnothing 12$ mm, the reduction changed.

Cold drawn inlet tubes, which were annealed, were used for the experiment. Tubes with a length of 3 m were cut to the required length of 500 mm. One end of each cutted tube was rotary swaged to a diameter of $\varnothing 11$ mm (the tube is gripped by the swaged end to the chuck of the tensile testing machine). The drawing speed was 60 mm / min. Molykote HTF Dispersion lubricating oil was used during drawing to reduce friction. A sketch of the shape and dimensions of the inlet tube is shown in Fig. 1.

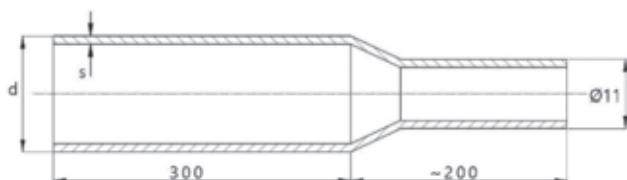


Fig. 1. The dimensions of the inlet tube

Rys. 1. Wymiary rury wlotowej

The tube material is low-carbon steel E235, which is suitable for the production of seamless tubes by cold drawing technology and is used in the automo-

tive industry, in the production of machine parts or in the production of tubes for pressure, hydraulic and pneumatic circuits.

The mechanical properties of E235 steel are as follows: Yield stress $R_e = \text{min. } 235$ MPa, tensile strength $R_m = (340\text{--}480)$ MPa, elongation $A_{\text{min}} = 25\%$. Low-carbon steel E235 has guaranteed weldability, good machinability and also hot and cold formability. The material used in the experiment was delivered after heat treatment, i.e. annealing ($890\text{--}950$ °C). The chemical composition of low-carbon steel E235 according to EN10305-1 is given in tab. 1.

Table 1. Chemical composition of steel E235 [wt %]

Tabela 1. Skład chemiczny stali E235 [% mas.]

Element	C	Si	Mn	P	S
Composition	0.170	0.350	1.200	0.025	0.025

For the purposes of the laboratory experiment, a special fixture was designed and manufactured to perform the technological experiments of the drawing of seamless steel tubes. The special fixture is structurally designed for clamping in the working space of the tensile testing machine. The clamping of the special fixture in the universal hydraulic tensile testing machine EU 40 is documented in Fig. 2. The drawing die (which shape and dimensions are shown in Fig. 3) was inserted into the base plate of the special fixture.



Fig. 2. Detail of the special fixture clamped in the universal hydraulic tensile testing machine EU 40

Rys. 2. Specjalny uchwyt zamocowany w uniwersalnej hydraulicznej maszynie wytrzymałościowej EU 40

Before the experimental drawing, the outer and inner diameters of the tubes were measured using the coordinate measuring machine ZEISS CenterMax and then the wall thickness of the tube before drawing was calculated. Coordinates measuring machines

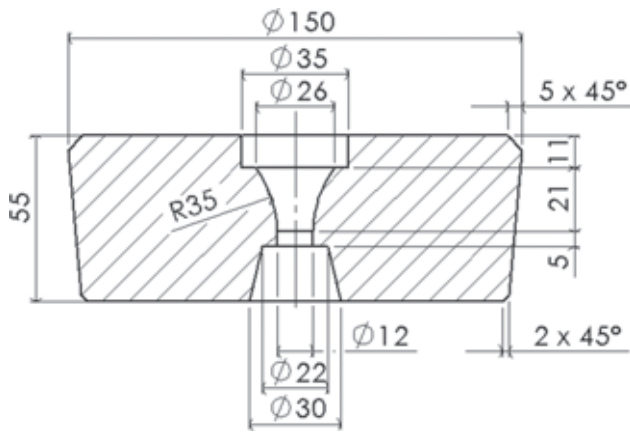


Fig. 3. Shape and dimensions of the drawing die
Rys. 3. Kształt i wymiary matrycy ciągnawej

system available to the CMM has a significant impact on the result of the measuring [17]. After drawing, the measurement of the outer and inner diameter of the drawn tube and the calculation of the wall thickness after drawing were also performed. The shape of the tube before and after drawing is shown in Fig. 4.



Fig. 4. The shape of the tube before and after drawing
Rys. 4. Kształt rury przed i po ciągnięciu

(CMM) enables measuring parameters with a high degree of accuracy, depending on the measuring method used and specific conditions. The scanning

Based on the measured tube diameters, it was possible to calculate the tube cross-sections and wall thicknesses before and after drawing. Reduc-

Table 2. Table of measured tube dimensions and calculated values (tube sinking, tube wall thickness 1 mm)

Tabela 2. Zestawienie zmierzonych wymiarów rur i obliczonych wartości (zanurzenie rur, rur of grubości ścianki 1 mm)

Steel E235	Sample no.	Outer tube diameter D_0 [mm]	Inner tube diameter d_0 [mm]	Outer tube diameter after drawing D [mm]	Inner tube diameter after drawing d [mm]	Wall thickness s_0 [mm]	Wall thickness after drawing s [mm]	Wall thickness differences Δs [mm]	Reduction R [%]
Tube diameter [mm] $\Phi 14$	4	13.971	11.952	12.009	9.832	1.009	1.088	0.079	9.2
	5	13.975	11.955	12.009	9.837	1.010	1.086	0.076	9.4
	6	13.977	11.958	12.013	9.848	1.009	1.082	0.073	9.6
Tube diameter [mm] $\Phi 16$	7	16.051	14.045	11.974	9.890	1.003	1.042	0.039	24.5
	8	16.053	14.047	12.016	9.840	1.003	1.088	0.085	21.2
	9	16.049	14.044	12.015	9.818	1.002	1.098	0.096	20.5
Tube diameter [mm] $\Phi 18$	1	17.993	15.953	12.016	9.895	1.020	1.060	0.040	32.8
	2	17.991	15.950	12.023	9.840	1.020	1.091	0.071	31.1
	3	17.994	15.955	12.019	9.878	1.019	1.070	0.051	32.2

Table 3. Table of measured tube dimensions and calculated values (tube sinking, tube wall thickness 2 mm)

Tabela 3. Zestawienie zmierzonych wymiarów rur i obliczonych wartości (zanurzenie rur, rur of grubości ścianki 2 mm)

Steel E235	Sample no.	Outer tube diameter D_0 [mm]	Inner tube diameter d_0 [mm]	Outer tube diameter after drawing D [mm]	Inner tube diameter after drawing d [mm]	Wall thickness s_0 [mm]	Wall thickness after drawing s [mm]	Wall thickness differences Δs [mm]	Reduction R [%]
Tube diameter [mm] $\Phi 14$	4	13.997	9.995	11.999	7.871	2.001	2.064	0.063	14.5
	5	13.992	9.998	11.994	7.897	1.997	2.049	0.052	14.9
	6	13.998	10.006	11.997	7.903	1.996	2.047	0.051	14.9
Tube diameter [mm] $\Phi 16$	7	16.015	11.931	11.986	7.771	2.042	2.108	0.066	27.0
	8	16.013	11.942	11.987	7.761	2.036	2.113	0.077	26.6
	9	16.020	11.951	11.997	7.654	2.035	2.171	0.136	25.0
Tube diameter [mm] $\Phi 18$	1	18.000	13.945	11.978	7.781	2.028	2.099	0.071	35.9
	2	18.032	13.977	11.999	7.658	2.028	2.170	0.142	34.2
	3	18.028	13.971	11.984	7.798	2.029	2.093	0.064	36.2

tion values were again calculated from the values of cross-sections. The wall thicknesses were used to calculate the change in tube wall thickness before and after drawing. The results of measuring the geometric dimensions of tubes before and after drawing are given in Tab. 2 and 3. The stated measured geometric dimensions were statistically evaluated and published in the paper [18]. From the measured and calculated results, the resulting tube wall thickness after drawing with the results obtained from the finite element method (FEM) simulation in the DEFORM software will be compared and evaluated.

3. COMPUTER SIMULATION OF DRAWING PROCESS USING SOFTWARE DEFORM

Computer simulation of the drawing process of E235 steel tubes was performed using the simulation software DEFORM-3D. It is a high-performance FEM simulation system for three-dimensional (3D) analysis of material flow in a wide range of forming processes. Simulation software is a practical and effective tool for prediction of plastic material flow in forming tools in order to reduce production costs and speed up the entire production process [7, 14, 19–21].

The pre-processing phase of the simulation requires modelling the tube semi-product, drawing

die and drawing carriage using CAD software. Furthermore, the models were imported into the software DEFORM in STL format. In the next setting of the FEM simulation, the following parameters were used: temperature of the semi-finished product and tool (drawing die) 25 °C, plastic material of the semi-finished product steel E235, drawing speed 60 mm / min, shear friction between the drawing die and the tube 0.08 and step increment 0.1 mm / step.

Furthermore, a tetrahedral network was generated on the semi-finished product and also the number of elements on the tube was selected. As the tubes had different diameters and different wall thicknesses, the number of elements was 182000 to 592000. The drawing die and drawing carriage were set as rigid.

The final phase of the computer simulation is called post-processing and allows to display the achieved results from the simulation of tube drawing. The aim of the contribution is to point out the use of post-processing results for mutual comparison of tube wall thicknesses with wall thicknesses values, which were measured after drawing in the laboratory experiment. Example of the display of the initial and final wall thickness of the tube after drawing obtained by computer simulation is shown in Fig. 5, 6, which also documents the histogram of the distribution and number of tube wall thicknesses.

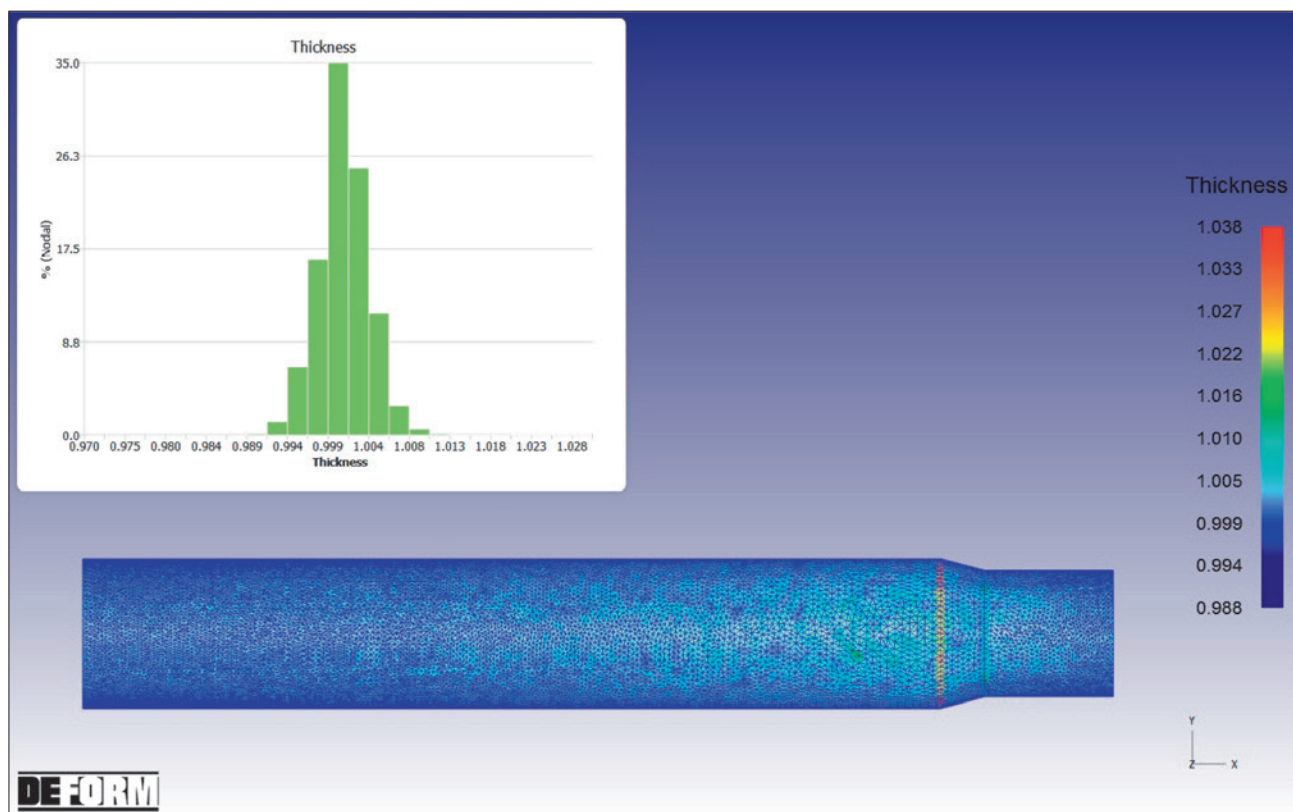


Fig. 5. Display of tube wall thickness before drawing obtained by computer simulation (Inlet tube with outer diameter of Ø14 mm with wall thickness of $s = 1$ mm)

Rys. 5. Obraz grubości ścianki rury przed ciągnięciem uzyskany za pomocą symulacji komputerowej (Rura wlotowa o średnicy zewnętrznej Ø14 mm i grubości ścianki $s = 1$ mm)

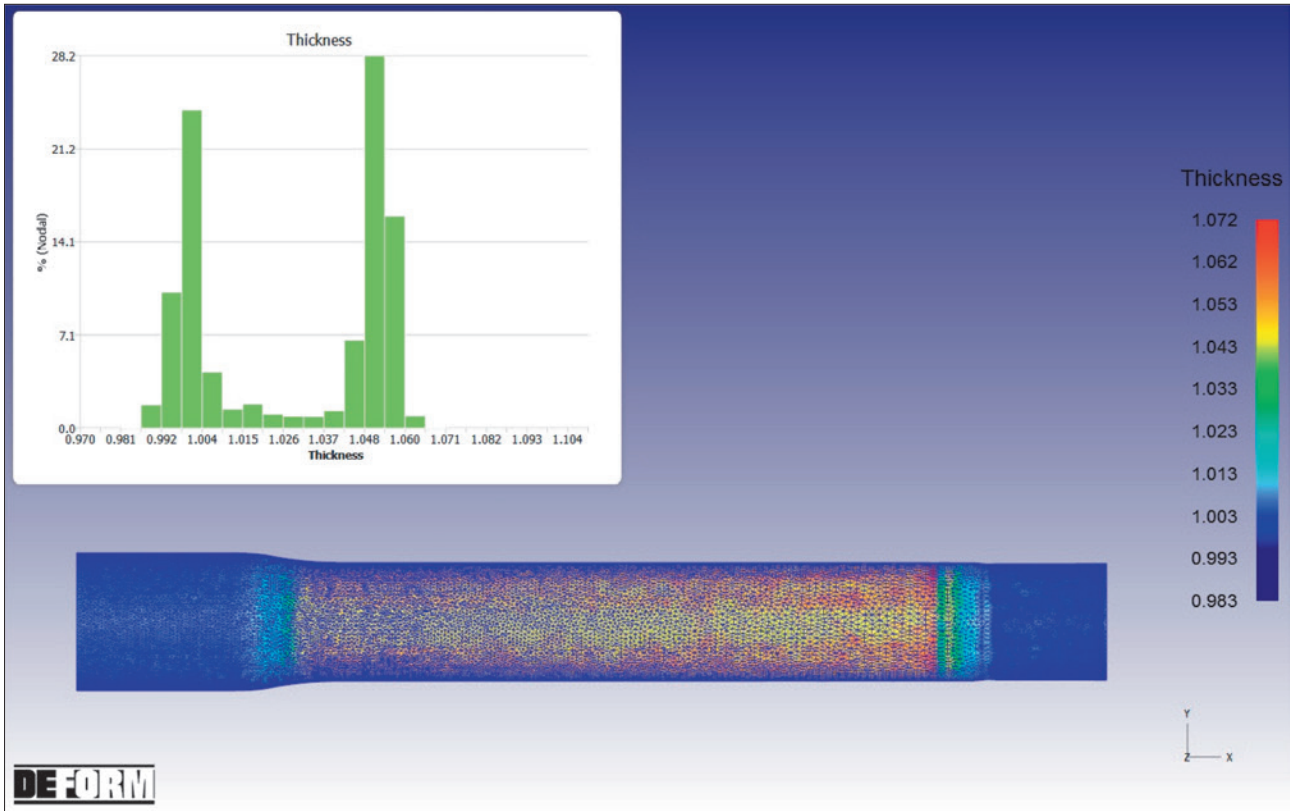


Fig. 6. Display of tube wall thickness after drawing obtained by computer simulation (Inlet tube with outer diameter of Ø14 mm with wall thickness of $s = 1$ mm)

Rys. 6. Obraz grubości ścianki rury po ciągnięciu uzyskany za pomocą symulacji komputerowej (Rura wlotowa o średnicy zewnętrznej Ø14 mm i grubości ścianki $s = 1$ mm)

4. ACHIEVEMENTS AND EVALUATION

The measured tube wall thicknesses before and after drawing from the experiment were compared with the results obtained from the simulation in the software DEFORM.

In FEM simulation of tube drawing, the inlet tubes had an outer diameter of Ø14, Ø16, Ø18 mm and the wall thickness of the tube was $s = 1$ mm and 2 mm.

All tubes were drawn to a final outer diameter of Ø12 mm using the single-pass drawing technology.

When displaying the resulting tube wall thickness in the software DEFORM (Fig. 6), the tip of the tube, which did not form, can also be seen, and there is also the end part of the tube, which did not drawn. Therefore, only the middle part of the tube after drawing was considered for a clear evaluation of the results. Subsequently, the tube wall thickness was

Table 4. Table of tube wall thickness in experiment and simulation

Tabela 4. Zestawienie grubości ścianki rury w eksperymencie i symulacji

Steel E235	Outer tube diameter [mm]	Experiment			Simulation		
		Wall thickness before drawing s_0 [mm]	Wall thickness after drawing s [mm]	Wall thickness differences Δs [mm]	Wall thickness before drawing s_0 [mm]	Wall thickness after drawing s [mm]	Wall thickness differences Δs [mm] min-max
Wall thickness 1 mm	Ø14	1.009-1.010	1.082-1.088	0.073-0.079	0.994-1.008	1.047-1.059	0.039-0.065
	Ø16	1.002-1.003	1.042-1.098	0.039-0.096	0.994-1.008	1.069-1.085	0.061-0.091
	Ø18	1.019-1.020	1.060-1.091	0.040-0.071	0.994-1.006	1.080-1.093	0.074-0.099
Wall thickness 2 mm	Ø14	1.996-2.001	2.047-2.064	0.051-0.063	1.989-2.020	2.045-2.071	0.025-0.082
	Ø16	2.035-2.042	2.108-2.171	0.066-0.136	1.989-2.018	2.059-2.080	0.041-0.091
	Ø18	2.028-2.029	2.093-2.170	0.064-0.142	1.989-2.015	2.054-2.078	0.039-0.089

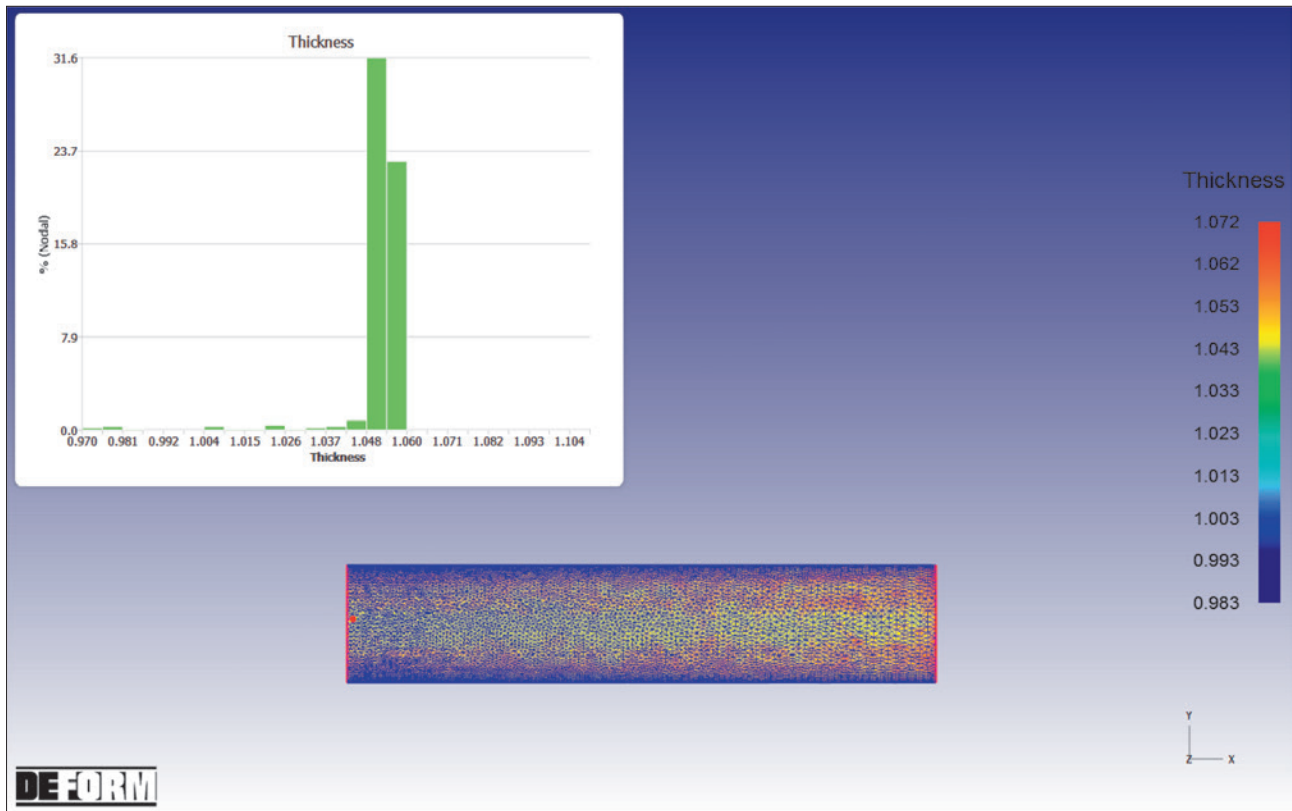


Fig. 7. Display of the wall thickness of the drawn tube after adjustment

Rys. 7. Obraz grubości ścianki ciągnionej rury po regulacji

displayed using a histogram in the post-processor of software DEFORM. The histogram shows the distribution and number of individual thicknesses in the volume of the tube (Fig. 7).

In this way, all drawn tubes in the simulations were adjusted and the wall thickness values of the individual examined tubes were obtained. These tube wall thicknesses are shown by the individual histograms in Fig. 8 and Fig. 9.

The comparison of the measured tube wall thicknesses from the tube drawing experiment with the tube wall thicknesses obtained in the simulation software DEFORM is shown in Table 4. The table also shows the calculated change in thickness Δs , which shows the difference between tube initial thickness and tube thickness after drawing. Experimental values of Δs were obtained from Tab. 2, 3. The values of the change in thickness Δs in the simulations were calculated from the ranges of values obtained from the individual histograms and are written in Table 4.

The following is an example of the calculation of the maximum and minimum possible change of the tube wall thickness Δs during the simulation (the example of calculation is for tube with outer diameter of $\varnothing 16$ and $s_0 = 1$ mm).

Tube thickness before drawings $s_0 = 0.994$ – 1.008 mm
 Tube thickness after drawing $s = 1.069$ – 1.085 mm
 Calculation of min $\Delta s = 1.069 - 1.008 = 0.061$ mm
 Calculation of max $\Delta s = 1.085 - 0.994 = 0.091$ mm

By this calculation was obtained the minimum and maximum possible change in tube wall thickness after drawing in the simulations.

The Tab. 4 shows that the changes in the tube wall thickness Δs measured in the tube drawing experiment and in the FEM simulations approximately are in the same ranges. Although there are some measured values from experiments that are at the upper limit compared to the simulations and other values are at the lower limit of this range Δs , which were obtained in the simulations. Most of the measured tubes are in the range of the change in the tube wall thickness, which were obtained by numerical simulation. It can be stated that the simulation results have a very good match with the wall thickness of the tube after drawing in the experiment. It follows from the above that in the future it would be necessary to have even more measured samples in the experiments for an even better evaluation and description of the results obtained from the experiment. In the experiment, it can be seen that the geometric input parameters of the tubes, and consequently the output parameters of the tubes, change significantly. As a result, the extent of the change in the tube wall thickness Δs then varies greatly from the results obtained in the simulations.

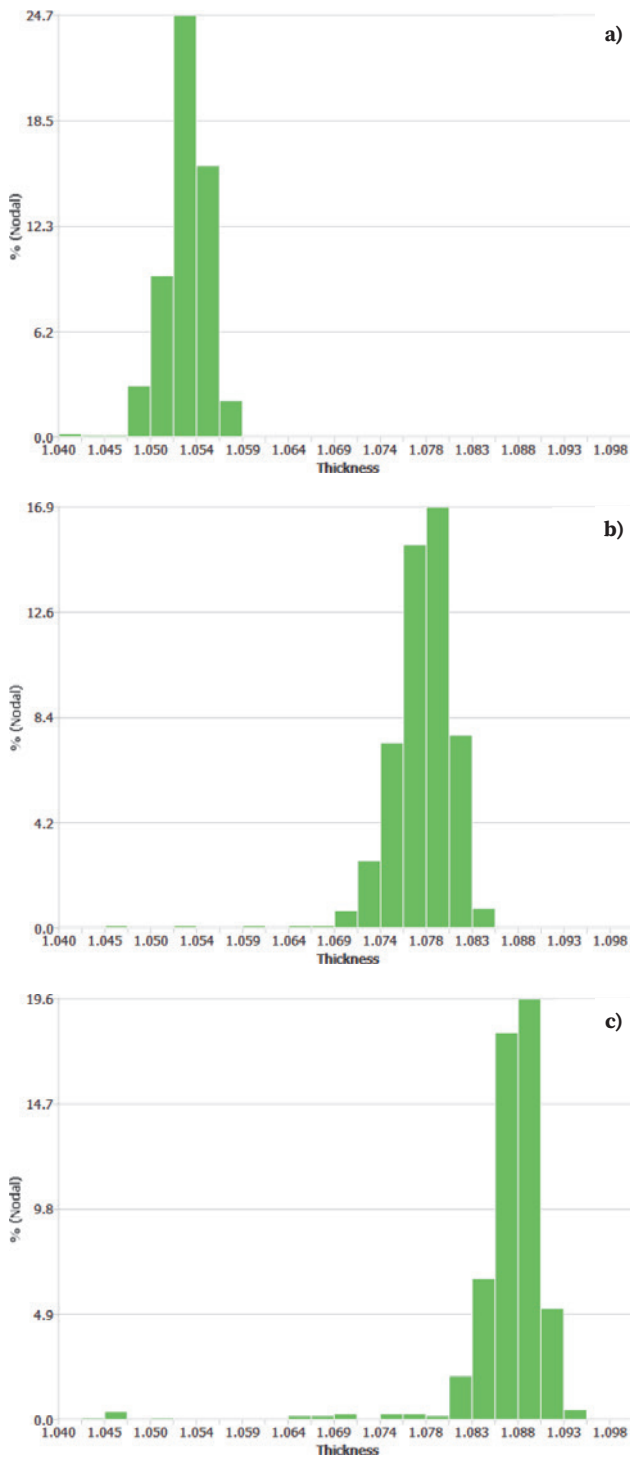


Fig. 8. Tube wall thickness after drawing for tubes with initial wall thickness of 1 mm: a) Ø14 mm, b) Ø16 mm, c) Ø18 mm

Rys. 8. Grubość ścianki rury po ciagnieniu dla rur o początkowej grubości ścianki 1 mm: a) Ø14 mm, b) Ø16 mm, c) Ø18 mm

5. SUMMARY

In conclusion, it can be stated that the tube wall thickness after drawing, which was obtained by simulation, has a very good match with the values of tube wall thicknesses obtained by measurement in tube experimental drawing. It was found that the change in tube wall thickness Δs is in the range of

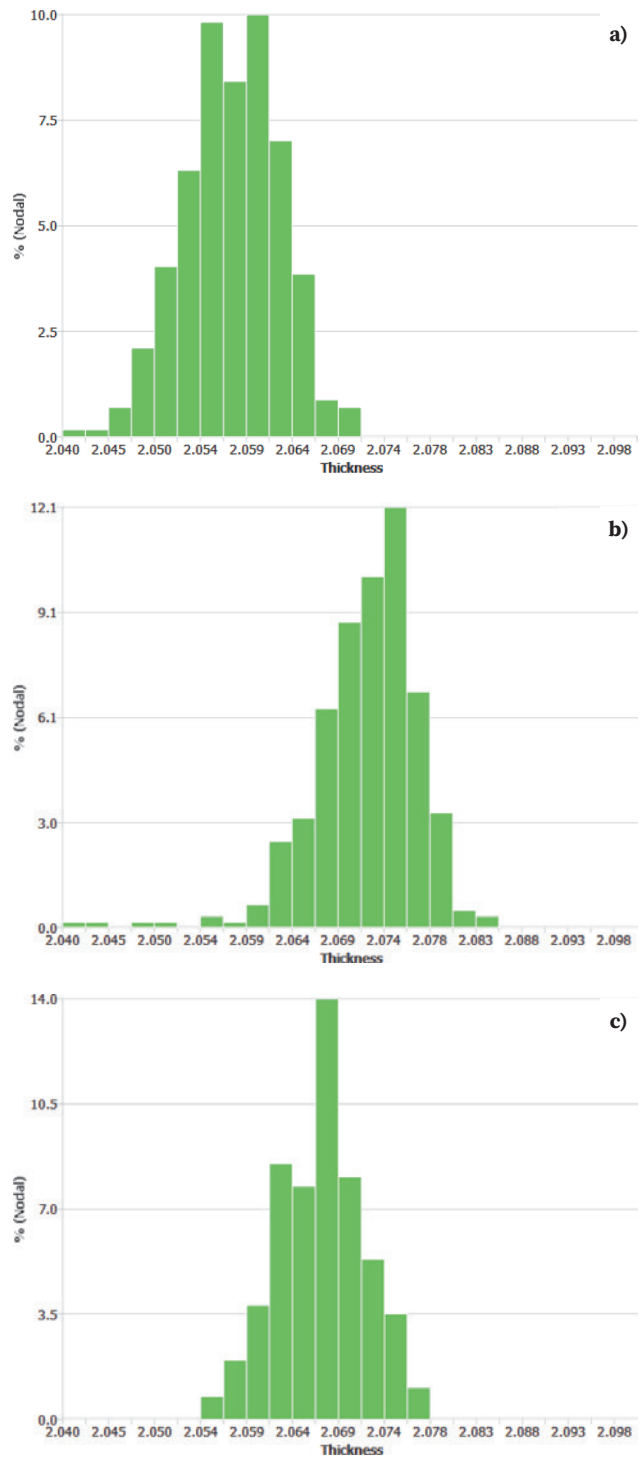


Fig. 9. Tube wall thickness after drawing for tubes with initial wall thickness of 2 mm: a) Ø14 mm, b) Ø16 mm, c) Ø18 mm

Rys. 9. Grubość ścianki rury po ciagnieniu dla rur o początkowej grubości ścianki 2 mm: a) Ø14 mm, b) Ø16 mm, c) Ø18 mm

0.040–0.090 mm, regardless of whether the tube wall thickness is 1 mm or 2 mm.

For the tube wall thickness of 1 mm, the variability of values is 4–9% and for the tube wall thickness of 2 mm, the variability of values is 2–4.5%, which is a sufficient tolerance in tube production, as the normal tolerance of tube wall thickness after tube drawing is +10%.

The accuracy of the measurement is influenced by the fact that in tube production plants, drawing often has a very different initial (input) tube wall thickness. This fact then also affects the resulting tube wall thickness after drawing.

Furthermore, from the analysis and comparison of the values obtained from the experiment and FEM simulation in the software DEFORM, it was found that the simulation software used is a reliable tool

for determining the exact dimensions and shape of tubes produced by cold drawing.

Acknowledgment

This work was supported by the Slovak Research and Development Agency under the Contract no. APVV-18-0418. (Research on causes of geometrical deviations in the production of seamless tubes and their technological inheritance with emphasis on the shape stability of precision cold drawn tubes using metrological systems).

REFERENCES

- [1] D. Radford, D.B. Richardson. *Production Engineering Technology*. 3 Ed. London: Macmillan publishers LTD, 1980.
- [2] W.F. Hosford, R.M. Caddell. *Metal Forming: Mechanics and Metallurgy*. 4 Ed. New York: Cambridge University Press, 2011.
- [3] M. Mojzis, L. Parilak, V. Tittel, M. Ridzoň, P. Bella, I. Buransky. Compare of the dies and they influence of geometry precision of the cold drawing tubes with small dimensions. *Hutnik – Wiadomości Hutnicze*, 2017, 84 (8), pp. 374-376.
- [4] R. Pernis. Calculation of wall thickness at tube sinking. *Acta Metallurgica Slovaca*, 2006, 12, pp. 191-201.
- [5] M. Palengat, G. Chagnon, D. Favier, H. Louche, C. Linardon, C. Plaideau. Cold drawing of 316L stainless steel thin-walled tubes: Experiments and finite element analysis. *International Journal of Mechanical Sciences*, 2013, 70, pp. 69-78.
- [6] F. Boutenel, M. Delhomme, V. Velay, R. Boman. Finite element modelling of cold drawing for high-precision tubes. *Comptes Rendus Mecanique*, 2018, 346 (8), pp. 665-677.
- [7] P. Bella, P. Bucek, M. Ridzoň, M. Mojzis, L. Parilak. Influence of die geometry on drawing force in cold drawing of steel tubes using numerical simulation. *Key Engineering Materials*, 2016, 716, pp. 708-712.
- [8] J.J. Sheu, S.Y. Lin, C.H. Yu. Optimum die design for single pass steel tube drawing with large strain deformation. In: *Procedia Engineering 81. 11th International Conference on Technology of Plasticity, ICTP 2014*, Japan, Nagoya Congress Centre, Nagoya, pp. 688-693.
- [9] S.K. Lee, M.S. Jeong, B.M. Kim, S.K. Lee, S.B. Lee. Die shape design of tube drawing process using FE analysis and optimization method. *The International Journal of Advanced Manufacturing Technology*, 2013, 66, pp. 381-392.
- [10] M.P. Groover. *Fundamentals of Modern Manufacturing*. John Wiley & Sons, Inc., 2010.
- [11] K. Sawamiphakdi, G.D. Lahoti, P.K. Kropp. Simulation of a tube drawing process by the finite element method. *Journal of Materials Processing Technology*, 1991, 27, pp.179-190.
- [12] J.Y. Acharya, S.M. Hussein. FEA based comparative analysis of tube drawing process. *Journal of Innovations in Engineering Research and Technology*, 2014, 1, pp. 1-11.
- [13] P. Bella, R. Durcik, M. Ridzoň, L. Parilak. Numerical simulation of cold drawing of steel tubes with straight internal rifling. *Procedia Manufacturing*, 2018, 15, pp. 320-326.
- [14] M. Kapustova, R. Sobota. The research of influence of strain rate in steel tube cold drawing processes using FEM simulation. *Novel Trends in Production Devices and Systems V (NTPDS V): Special topic volume with invited peer reviewed papers only*. Zurich: Trans Tech Publications, 2019, pp. 235-242.
- [15] G. Kumar Mishra, P. Singh. Simulation of Seamless Tube Cold Drawing Process using Finite Element Analysis. *Journal for Scientific Research & Development*, 2015, 3, pp. 1286-1291.
- [16] P. Karnezis, D.C.J. Farrugia. Study of cold tube drawing by finite-element modelling. *Journal of Material Processing Technology*, 1998, 80-81, pp. 690-694.
- [17] J. Moravcikova, P. Pokorný. The influence of machine-part measuring strategies for coordinate measuring devices on the precision of the measured values. *Acta Polytechnica Hungarica*, 2018, 15 (6), pp. 7-26.
- [18] L. Morovic, M. Kritikos, D.R.D. Sobrino, J. Bilik, R. Sobota, M. Kapustova. A Statistical Approach in the Analysis of Geometrical Product Specification during the Cold Tube Drawing Process. *Applied Sciences*, 2022, 12 (2), pp. 1-22.
- [19] P.M. Dixit, U.S. Dixit. *Modeling of Metal Forming and Machining Processes by Finite Element and Soft Computing Methods*. London: Springer Verlag, 2008.
- [20] S. Kobayashi, S.I. Oh, T. Altan. *Metalforming and the Finite-Element Method*. London: Oxford University Press, 1989.
- [21] M. Kapustova, R. Sobota. The design of drawing process of cylindrical cup with oval bottom using computer simulation. In *MATEC Web of Conferences. ICMME 2016*. Shanghai, 2017, p. 95.